*metals*

MDPI

*Article*

# Design Implications and Opportunities of Considering Fatigue Strength, Manufacturing Variations and Predictive LCC in Welds

**Mathilda Karlsson Hagnell [1,*,†], Mansoor Khurshid [2,3,†], Malin Åkermo [3] and Zuheir Barsoum [3,*,†]**

[1] The Centre for ECO2 Vehicle Design, KTH Royal Institute of Technology, Teknikringen 8, 10044 Stockholm, Sweden
[2] Cargotec Sweden AB Bromma Conquip, Kronborgsgränd 23, Box 1133, 16422 Kista, Sweden; mansoor.khurshid@bromma.com
[3] Lightweight Structures, Engineering Mechanics, KTH Royal Institute of Technology, Teknikringen 8, 10044 Stockholm, Sweden; akermo@kth.se
* Correspondence: mathk@kth.se (M.K.H.); zuheir@kth.se (Z.B.)
† These authors contributed equally to this work.

**Abstract:** Fatigue strength dictates life and cost of welded structures and is often a direct result of initial manufacturing variations and defects. This paper addresses this coupling through proposing and applying the methodology of predictive life-cycle costing (PLCC) to evaluate a welded structure exhibiting manufacturing-induced variations in penetration depth. It is found that if a full-width crack is a fact, a 50% thicker design can result in life-cycle cost reductions of 60% due to reduced repair costs. The paper demonstrates the importance of incorporating manufacturing variations in an early design stage to ensure an overall minimized life-cycle cost.

**Keywords:** manufacturing variations; life-cycle costing; fatigue assessment; welding; welding defects



**Citation:** Hagnell, M.K.; Khurshid, M.; Åkermo, M.; Barsoum, Z. Design Implications and Opportunities of Considering Fatigue Strength, Manufacturing Variations and Predictive LCC in Welds. *Metals* **2021**, *11*, 1527. https://doi.org/10.3390/met11101527

Academic Editor: Pierpaolo Carlone

Received: 27 August 2021
Accepted: 21 September 2021
Published: 26 September 2021



## 1. Introduction

Service interruption due to premature fatigue failure in welded joints can result in significant operational and monetary losses. As premature fatigue failures are often a result of initial manufacturing defects and their variation, as shown by [1], both must be accounted for in the design process. In addition, a structure must also be produced and operated at a competitive cost level, which means life-cycle costing must also be part of the design equation in order to ensure an optimal design.

In a welded joint, fatigue failure is often a result of cracks initiated at the weld toe or the weld root, respectively [2–4]. When a welded joint fails from the root, the fatigue resistance has been found to be affected by several geometrical variables such as weld throat size, plate thickness and depth of weld penetration [5,6]. All these geometrical variables are in turn influenced by manufacturing and variations, and can therefore introduce defects and variations that ultimately govern the final fatigue performance of any particular weld [1]. Strategies to ensure weld qualities are numerous, ranging from weld procedure recommendations [2] to the introduction of post-weld treatments such as HFMI, TIG and burr-grinding [7–9] or post-weld thermal treatments [10,11]. However, all these mentioned quality-ensuring strategies comes at an increased manufacturing cost. A cost, which ultimately has to be compared to that of increased fatigue lifetime, and hopefully reduced operational costs.

Apart from technical capacity, the fatigue design of a structure also dimensions its full life-cycle cost (LCC), and life-cycle energy impact. For example, a design with an improved fatigue behaviour is likely to become more costly to produce as it may include more expensive materials; and/or results in a more involved production process. However, the same design would become less costly throughout its operational use due to its longer technical life and potentially lower maintenance and repair need. Consequently, to fully

control and balance both fatigue and life-cycle cost, fatigue assessment and life-cycle cost should ideally be done simultaneously in an early conceptual design stage.

Advances in cost modelling [12–14], have shown that there exists an increased interest in introducing cost assessments in an early design stage. However, life-cycle analysis (LCA), and a traditional LCC, is ultimately still performed in a later design stage as it requires extensive material flow knowledge and large databases. Answering to this, recent research has come to highlight the design benefits of adapting a simplified, more generalized, early-stage LCA. In the study by [15], the method of life cycle energy optimization is proposed and shown useful to assess the importance of recycling of lightweight composite materials. In [16], the authors present a material-selection approach that incorporates both structural design and LCA that spans material systems. In the study by [17], LCA-optimization of a concrete precast bridge provides essential design guidance in relation to the found energy-intensive life-cycle stages of manufacture, use and maintenance. Moreover, for steel bridge construction, Ref. [18] finds that simple production cost optimization leads to increased life-cycle cost. This underlines the importance of designing for full life-cycle cost as opposed to that of only production cost. In addition, LCC is often incorporated in work available on maintenance and repair logistics and optimization, such as work by [19–22]. However, when it comes to LCC coupled to manufacturing variations and fatigue assessment of welded structures, the scientific literature of the field becomes limited. Hence, more research is needed.

This motivates the current study, where the gap is addressed through proposing a predictive LCC (PLCC) scheme, that predicts production, use and end-of-life (EoL) costs of welded structures as a function of governing geometry, complexity and required production and recycling flows. Here, predictive means that the methodology is aimed for use in an early conceptual design stage, in which it can identify general trends that supports holistic design decision while demanding a low amount of user input. Involved production costs are estimated through implementing a previously developed predictive technical cost model by [12,23].

The PLCC scheme is implemented and demonstrated in a parametric case study in which the thicknesses of the main load-carrying members of a representative welded box structure are varied. The different plate thicknesses give rise to different fatigue strength properties and ultimately also different life-cycle costs. Two different fatigue scenarios are considered, each representative of a specific manufacturing variation with respect to lack of penetration depth (LOP). LOP is chosen as a representative manufacturing defect due to its importance to ensure full fatigue life, as shown by [24]. To further assess the production cost impact of penetration depth, an additional assessment of the production cost as a result of penetration depth of the structure is presented. Finally, a discussion is presented on general aspects on managing variations in welding, their impacts on fatigue life as well as important aspects on overarching design related to fatigue assessment methods. Overall, the study spans disciplines on cost and fatigue assessments and addresses important aspects on the multi-disciplinary problem of designing cost-efficient, and robust, welded structures.

## 2. Scope

The methodology and case-study presented in this paper connects conceptual design of welded fatigue-dimensioned structures to lifecycle costing (LCC). As the focus is early conceptual design, the definition of predictive lifecycle costing (PLCC) is introduced. The methodology suitability is evaluated for application in a variation-driven conceptual design stage. Consequently, discussions on the impact of variation-driven issues with regards to fatigue and predicted life cycle cost are also given as part of the results.

Given the focus on conceptual design, or early stage development, a number of assumptions and limitations need to be posed in order to complement the inherent lack of design knowledge present in such early design stages. Assumptions and limitations include:

- A traditional lifecycle assessment include present distribution channels. However, for the scope of this study, distribution is deemed too uncertain to assess at an early design stage.
- Input cost data such as material cost per kg and equipment investments are retrieved from comparative, published, data to avoid assessing the result of specific supply-chains and internal business partnerships.
- Investment costs are sized for full use in specific production, this means shared equipment systems are not included.
- R&D and overhead costs are excluded from the modelling scope as they are highly tied to specific organizations and often difficult to credit any particular component.
- Inspection and control are not treated in this work, but are instead part of future work.

## 3. Methodology and Framework

To couple PLCC and conceptual design of fatigue-designed welded joints, it is important to understand, and model, the existing connections and variables between the two. Examples of important variables that connect fatigue performance and individual lifecycle phases are illustrated in Figure 1. The individual coupling variables can either align or converge on life-cycle cost and fatigue behaviour with regards to their optimal value. For example, a low-cost material type minimizes material cost, but likely has an adverse effect on fatigue performance. This in turn affects not only material cost, but also consecutive use phase cost. To further increase the design complexity, the full design space involves a multitude of variables, all with different impact on fatigue behaviour and life-cycle phases. Note that the illustration in Figure 1 lists a full set of connections and variables and depending on specific study, some may not be meaningful in individual cases. For example, for a full structure or a mixed-material system; end-of-life costs are a function of involved geometries as end-of-life disassembly grows in complexity the more complex a geometry or connective welds are. In contrast, end-of-life costs of a single material slab require no disassembly, thus rendering the variable connection unimportant.

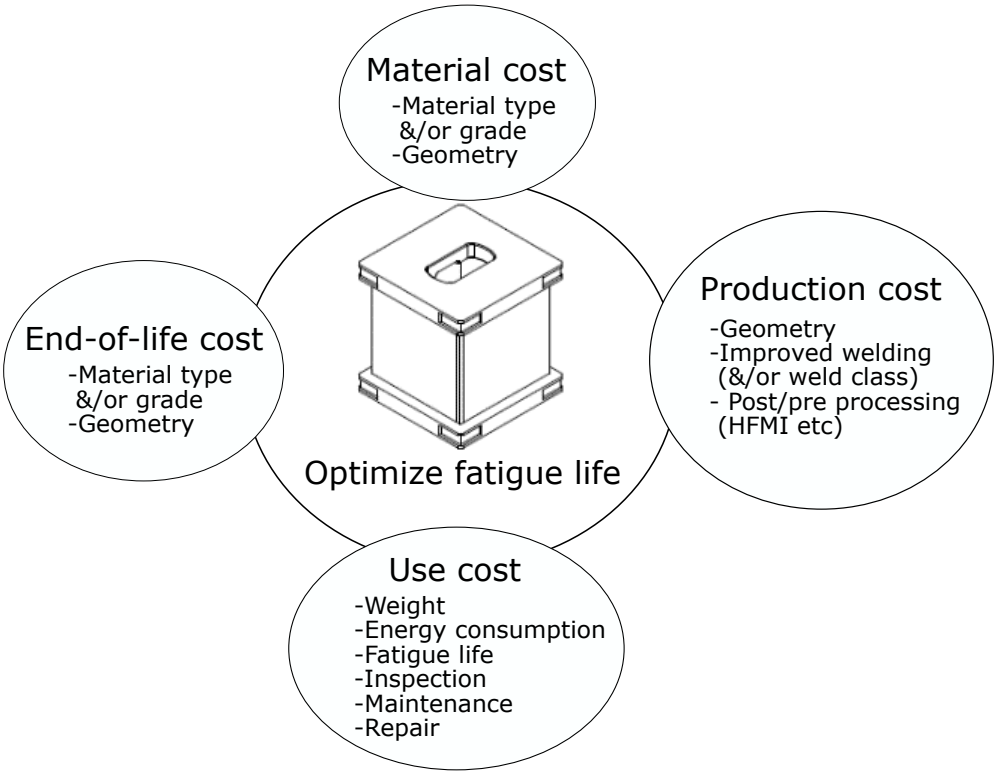


**Figure 1.** The coupling between LCC and fatigue-dimensioned welded components can be expressed through variables that connects the two for considered life-cycle phases.

## 4. Predictive Lifecycle Costing (PLCC)

The current study addresses the impact of four life-cycle phases, presented in Figure 2. These phases are raw material acquisition, component production, component use and finally component end-of-life. The life-cycle is considered to be an ideal closed material loop [25], which means that a certain percentage of the entering material is assumed to be recycled to new steel material of the same grade and re-used in a product within the same life-cycle flow. This closed-loop assumption is justified by the fact that steel produced and recycled through an electric arc furnace (EAF) process can be fueled by 100% scrap material [26]. This means that in theory, all scrap material produced during the steel's life-cycle can be recycled. However, as the quality of EAF produced steel is affected if fed by a scrap steel mix containing to many impurities [27], a retrieval rate of 80% is assumed. The material and production costs of a studied component is estimated using a previously developed predictive technical cost model [12,23], while the use phase and end-of-life phase costs are evaluated separately.

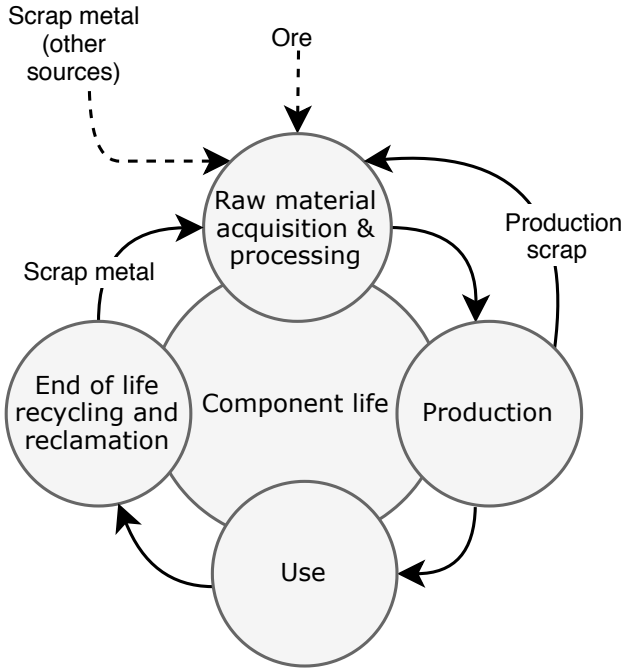


**Figure 2.** Simplified lifecycle applied within the scope of this paper. Note that a closed loop material flow is assumed, which means dashed material flows (scrap metal originating from other sources and ore) are only drawn for illustrative purposes, and not considered in the following case-study.

## 5. Predictive Technical Cost Model

To estimate material and production costs of studied component, a previously developed predictive technical cost model [12,23,28] is applied. The model is developed as a stand-alone package in Python [29] and estimates cost through connecting specified production flow to component geometry and complexity [12,23], see Figure 3. The cost model is modular and the production flow is defined by the user through configuring and combining necessary process steps involved in sought production method. The full cost is calculated as the sum of material costs and costs involved within each production process step. Cost categories considered within the scope of the model are defined in Figure 4. Indirect costs such as R&D development and overhead costs are not included within the scope of this model as their size are highly individual and often not known in an early design stage. For the scope of this paper, some extensions to the model library have been made in order to include that of necessary metallic production, including welding processes.

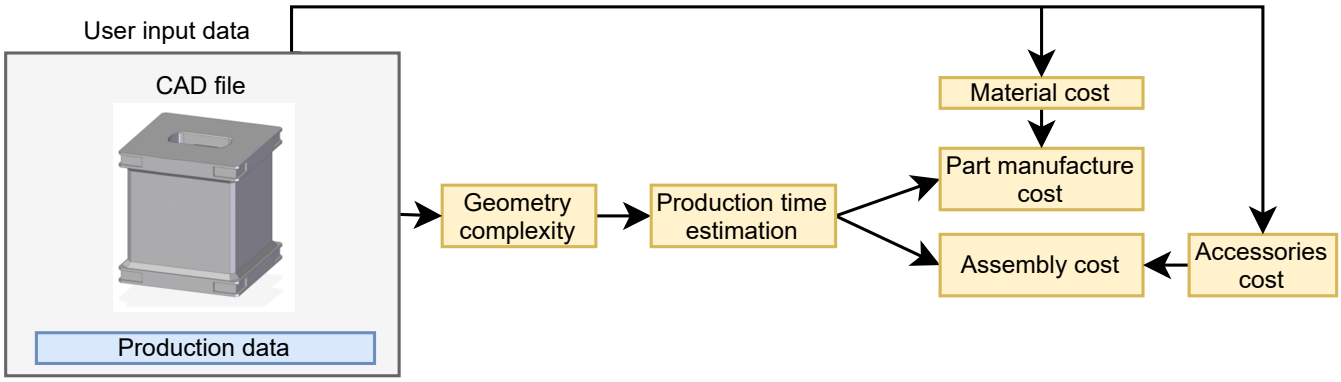


**Figure 3.** Information flow in applied predictive technical cost model, adapted from previous work [12].

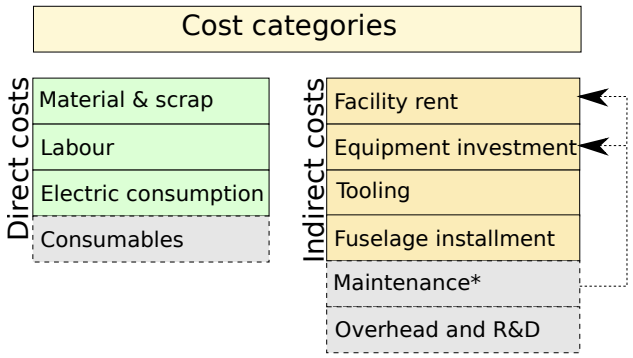


**Figure 4.** Considered direct and indirect cost categories (drawn in bold line) include material and scrap, labour and power consumption costs. Neglected costs (drawn in dashed line) are overarching costs, such as overhead and R&D, as well as pure consumables (for example basic safety equipment such as gloves, etc). Maintenance costs are not explicitly calculated, but are an implicit part of set equipment utilization and facility costs [28].

### *5.1. Geometry Complexity*

Component complexity is directly correlated to manufacturing and its cost, as the more complex, the more difficult and costly it becomes to manufacture. In the python package, the geometry complexity of the structure to be assessed is calculated and expressed through a complexity factor, C. As a CAD-geometry generally is described using point-clouds and bounding faces, the complexity factor is determined for each such individual bounding face. Factors considered for each bounding face include the face angle, the face curvature radius and the overall face curvature degree. The face angle is the largest internal or neighbour angular transition to the face centre normal. The face curvature radius is the corresponding radius $1/\kappa$ of either the current face, or that neighbour face depending on which produces the highest angular transition. The overall face curvature degree is either single or double, representing a surface bending in single axis versus two axis directions. For more details, see [23].

### *5.2. Production Time Estimation*

Process time is estimated as a function of production process. In general, processing times of machining or additive manufacturing and assembly steps are estimated as a function of the processing rate, $r$, component complexity, and governing characteristic size, $L$ according to [23] as

$$t = \frac{L}{rC} \tag{1}$$

5.2.1. Machining

Machining of metallic parts are performed using a 5-axis CNC-machine. Machining time is a function of cut length, $L_c$ and table feed rate, $v_f$, according to [30] as

$$t = \frac{L_c}{v_f} \tag{2}$$

where the table feed rate range from 100 to 250 m/min depending on steel grade [31]. Given the circular cut tool radius of $r$, each table feed motion removes up to $\pi r^2$ m$^2$ of material per $r$ m feed. An approximation of the removal rate of a face cut-out is therefore

$$Q_A = \frac{A_c}{r v_f}, \tag{3}$$

where $A_c$ is the cut tool area. Using a cut tool of $\phi$ 15 mm and a table feed rate of 250 m/min, the resulting face removal rate is approximately 0.1 m$^2$/s. This means the approximate machining time of a face cut-out can be calculate similarly to Equation (2), as $t = A_c/Q_A$.

5.2.2. Welding

For welding methods using solid wires such as metal arc welding (MAG) (ISO 4063-135) and flux cored arc welding (FCAW) (ISO 4063-136), it is proposed that the time to weld a joint between two parts can be expressed as

$$t_{prep} + t_{tack} + t_{pass} + (no_{passes} - 1)t_{repos} + t_{refill} n^{\circ}{}_{wires} + t_{post} \tag{4}$$

Variables included are the weld preparation time, $t_{prep}$, the time to tack weld the plates to achieve sufficient stability for upcoming weld process, $t_{tack}$, the number of weld passes, $no_{passes}$, the actual weld pass time, $t_{pass}$, the time that the welder needs to reposition the wire electrode in between passes, $t_{repos}$, the solid wire refill time, $t_{refill\ wire} no_{wires}$ and finally the weld post-processing time, $t_{post}$.

The weld pass time is a function of bead mass, $m$, and deposition rate, $r_w$, according to [32] as

$$t_{pass} = \frac{m}{r_w} \tag{5}$$

The bead mass depends on the weld cross-sectional area, $A_{bead\ weld}$, and is here approximated as half of an ellipse and is a function of throat thickness, $a$ and penetration depth $i$, see Figure 5.

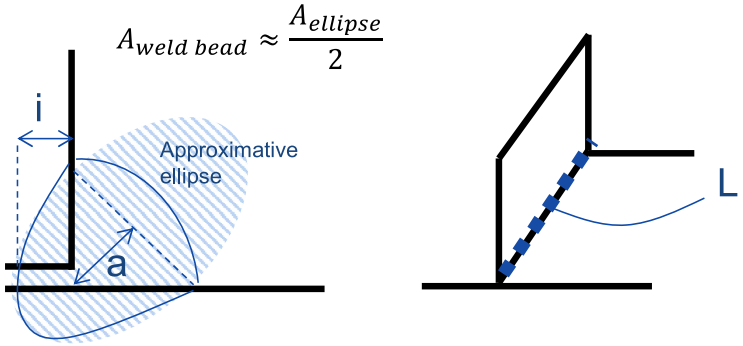


**Figure 5.** The weld bead mass is calculated from an assumed elliptical cross-sectional area, which is a function of throat thickness, $a$ and penetration depth $i$.

The deposition rate is a function of the electrode area, $A$, weld metal density, $\rho_{weld\ metal}$, wire feed speed, $v_{feed}$, and deposition efficiency, $\eta$, and can be expressed as [32]

$$r_w = A \rho_{weld\ metal} v_{feed} \eta \tag{6}$$

The wire feed speed, $v_{feed}$, can be preliminary determined as a function of weld method and weld complexity [33], if not directly stated by a comparable specified weld process specification (WPS). The deposition efficiency, $\eta$, is also a function of welding method and is 0.95 and 0.85 for MAG and FCAW 0.85, respectively [32].

The reposition time, $t_{repos}$, need to be at least that of the pass cooling time, $\Delta_{t8/5}$, which can be calculated as a function of the preheat temperature, $T_0$, and the gross heat input per unit length of weld kJ/mm, $q_w$ according to [34] as

$$\Delta_{t_{8/5}} = (6700 - 5T_0)q_w(\frac{1}{500 - T_0} - \frac{1}{800 - T_0}) \quad (7)$$

5.2.3. Weld Preparation

Weld preparation can consist of different processes such as gouging [32], manual abrasive cleaning or the application of a chemical cleaner. In general, the time to perform these type of processes is proposed to be expressed as a function of the weld length, $L$, the weld leg hypotenuse, $b$, the process speed, $v$, and the weld complexity factor, $C_w$, according to

$$t_{prep} = bLvC_w \quad (8)$$

In an early conceptual stage, the complexity factor, $C_w$, can be assumed equal to that of a difficulty factor as suggested by [33].

### *5.3. Material Cost*

The material cost is calculated as a function of the scrap rate, $r_{scrap}$, cost per kg material, $C_{kg\ cost}$, and the weight of the component, $w$, according to [23] as

$$C_{mtrl\ cost} = wC_{kg\ cost}(1 + r_{scrap}) \quad (9)$$

The cost per kg material is usually negotiated with respect to purchased quantity and supplier relationship status; however, as the cost model is to be applied in an early stage conceptual phase, guiding price indexes such as that of steel price index figures [35] and other material data bases [36] are used throughout the model.

### *5.4. Part Manufacture Cost*

Direct costs such as labour and power consumption are a function of individual cost driver, i.e. hourly cost and electricity cost respectively, and process time $t$. Indirect costs such as facility rent, equipment investment and tooling are calculated as a function of manufacturing volume, $n$, or parts per year. Necessary number of facility and production lines, $n_p$, are therefore calculated as a function of process time, annual work time, $t_{tot}$ and the annual production volume according to [23] as

$$n_p = \left\lceil \frac{tn}{t_{tot}} \right\rceil \quad (10)$$

Given Equation (10), the investment cost of a certain manufacturing method is calculated as $n_pC_I/\delta$, where $C_I$ is the investment cost of a piece of equipment and $\delta$ its depreciation rate. To account for installation and drive-in costs, an extra 20% is added to the investment cost of acquired machinery.

Machining

The investment cost of a CNC-machine can vary from 50 k€ for a 2-axis-machine to beyond 500 k€ for a multi-spindle, multi-axis machine [37]. A 5-axis CNC-machine for 300 k€ is considered to fulfil most needs and feed speeds for a medium to high production setup [23].

### *5.5. Assembly Cost*

The predictive technical cost model covers several different assembly processes, both manual and automatic. The assembly method of importance for a later case study is that of metallic welding.

Metal Arc Welding and Flux Cored Arc Welding

The investment cost of a welding machine varies from 700 € for a small 140 A manual welder to 17 k€ for an industrial-graded 600A synergic welder [38]. In the predictive technical cost model, welding equipment is selected based on sufficient power output for manual or synergic, see Figure 6. A manual welding machine demands a more skilled operator, but is generally less costly than a synergic, or pulse-controlled, machine.

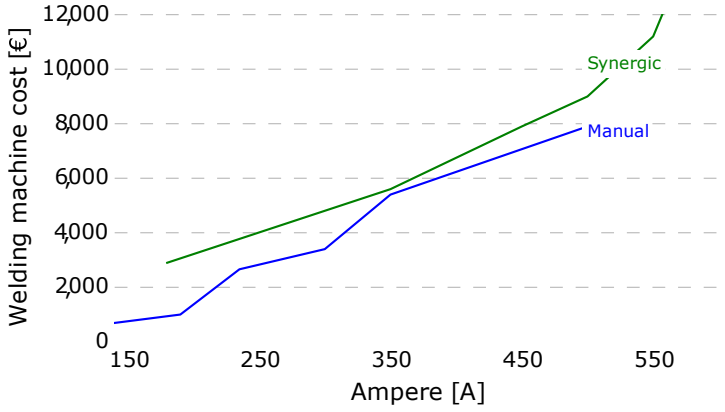


**Figure 6.** Investment costs of different welding machines [38,39] as a function of highest Ampere output.

## 6. Fatigue Assessment

Apart from manufacturing variations, fatigue assessment in itself give rise to hidden design variations as different fatigue assessment strategies yield different fatigue strength. In fact, a design can become either under-performing or overly conservative if the chosen fatigue life assessment strategy is not sufficient for the particular design and loading scenario.

Currently, there are mainly four established methods for fatigue life assessment of welded structures [2–4]; nominal stress approach, structural/geometrical "hot-spot" stress approach, effective notch stress approach and linear elastic fracture mechanical crack growth approach. Fatigue resistance of complex welded components based on stress analysis performed with FEA can be assessed in many ways with varying degrees of time consumption and accuracy. A large model will increase both the model preparation and the computational time. Large and complex FEA models may include several critical locations and complex boundary conditions, see example in Figure 7 where the stress value is continually changing at different locations. Nominal stress values are in some of the critical sections difficult or impossible to define. Even if a nominal stress can be defined, one must select from a catalogue of details, the geometry most closely resembling the actual welded detail. In many cases, the actual weld has little similarity to one of the geometries shown in the standards [40–42]. A schematic overview over complexity and work effort for different design methods are presented in Figure 8.

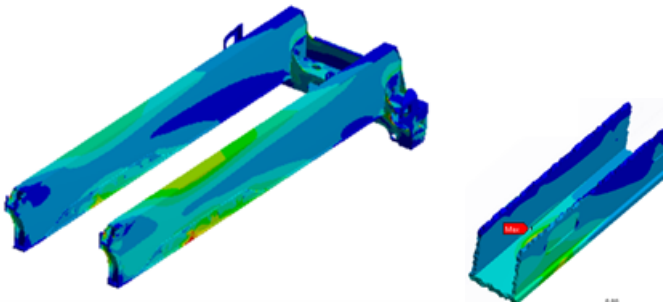

**Figure 7.** Stresses in Telescopic beam unit of a spreader, red colour corresponds to high and blue to low stresses.

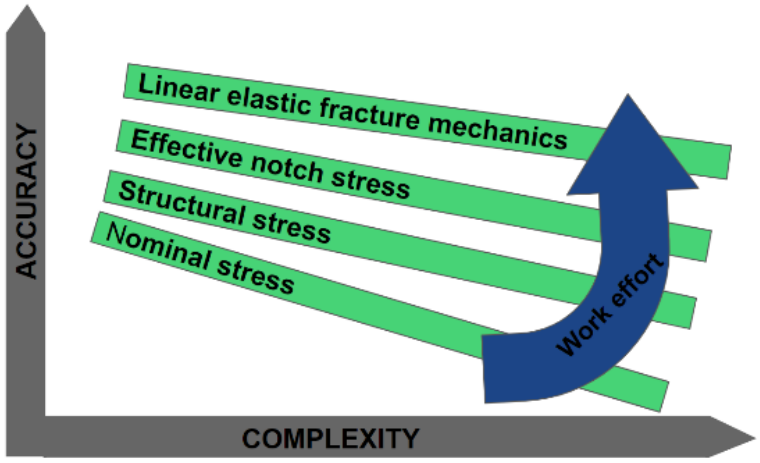


**Figure 8.** Schematic overview accuracy, complexity and work effort associated with the different fatigue assessment methods for welded structures.

Various studies have been conducted in order to investigate the accuracy and to map the source of variation for these different fatigue assessment methods. Ref. [43] carried out fatigue assessment using conventional methods and compared the results with fatigue testing of welded A-stay beam structure in an articulated hauler. The failure observed was weld root failure, and it was observed that the estimated fatigue life showed large scatter.

In a recent study, Ref. [44] carried out a round robin fatigue strength assessment of the welded box structure, identical to the structure investigated in the current study. The aim of the study was to identify variation and sources of variation in welding production, map scatter in fatigue life estimation and define and develop concepts to reduce these in all steps of product development. The estimated fatigue lives were also compared with fatigue testing, where the objective was weld root failure where different amounts of weld root penetration were studied. Differences were identified between both methods and participants using the same code/recommendations. It was concluded that for the applied cases, the nominal stress method overestimated the fatigue life and the effective notch method is conservative in comparison to the life of tested components.

Delkhosh et al. [45] studied the fatigue strength of the component in this study using Linear Elastic Fracture Mechanics (LEFM) approach. A parametric study was conducted to study the effect of various weld parameters on the fatigue strength, such as lack of weld metal penetration, load position, and plate thicknesses. The LEFM approach could capture the crack propagation from the weld root reasonably well and estimate the fatigue life. It was observed that compared to fatigue life estimations by nominal stress method or effective notch stress method, the LEFM approach could estimate the residual life more accurately, see Figure 9.

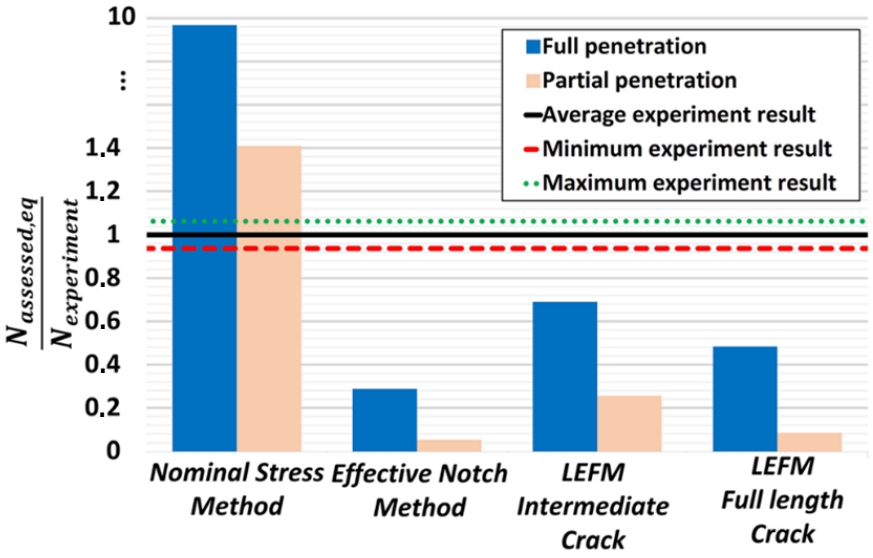


**Figure 9.** Results range for the different methods and level of the fatigue life assessed, from [45].

Residual stresses in welded joints can have beneficial or detrimental effect on the fatigue strength [2–4]. Residual stresses in the box welded structure considered in this study were evaluated experimentally and numerically by [46]. The effect of residual stress state on the fatigue strength of box welded structures has been discussed by Delkhosh et al. (2020). It was concluded that residual stresses did not significantly affected the fatigue strength of the box welded structure.

## 7. Case Study: PLCC of a Welded Box Structure

The investigated structure is a representative welded box structure, see Figure 10. The structure is an important member in a spreader. The box structure consists of two flange plates and four web plates [45]. The plates are manufactured from high-strength-structural steel (HSS) where the flange plates are manufactured from S700QL, a quenched and tempered grade, while the web plates are manufactured from S600MC, a hot-rolled structural steel made for cold forming. The structure is assembled through four longitudinal welds and two circumferential bevel welds, see Figure 10. From the perspective of fatigue, the circumferential bevel welds are the critical welds.

Parameters investigated in the PLCC case study include varied flange plate thickness, $t_f$, varied web plate thickness, $t_w$ and off-center hole position. Design cases and parameter configurations of current case study are given in Table 1. Note that the shift of the hole position, 30 cm towards the critical web plate, effect the symmetry of the loading. This causes the loading mode to become eccentric and thus effects the fatigue life of the box.

**Table 1.** Design cases and parameter values [45].

| Specimen Group | Case ID | Flange Thickness $t_f$ [mm] | Web Thickness $t_w$ [mm] | Loading Mode |
|---|---|---|---|---|
| Reference case | MTA | 30 | 10 | Centric |
| Varied $t_f$ | MTB | 40 | 10 | Centric |
| | MTC | 60 | 10 | Centric |
| Varied $t_w$ | MTD | 30 | 8 | Centric |
| Varied hole position | MTE | 30 | 10 | Eccentric |
| | MTF | 40 | 10 | Eccentric |

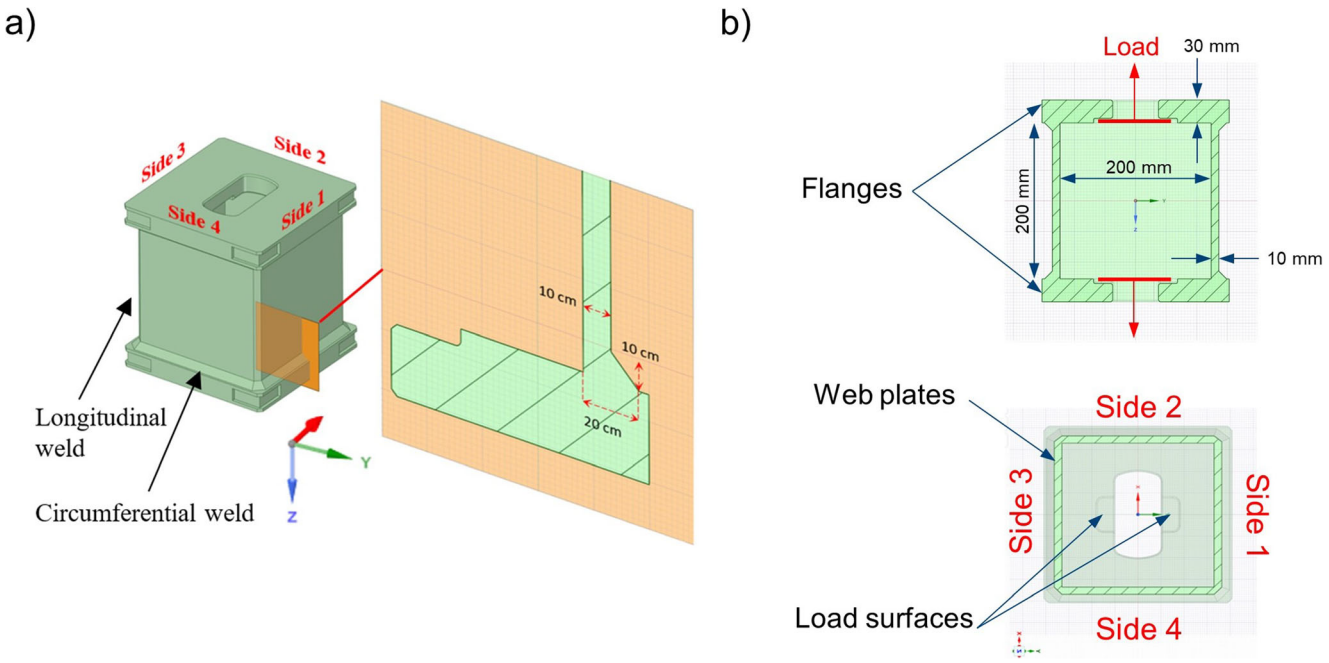


**Figure 10.** The welded box structure in (**a**) and applied load and dimension details in (**b**) [45].

### *7.1. Fatigue Behavior and Estimated Life*

Each weld box design case is evaluated with respect to four fatigue scenarios of different severity, see Table 2. In each fatigue scenario, it is assumed that the welded box fails as a result of LOP. Note that full weld penetration in this case still assumes a slight lack of penetration of 0.5 mm.

**Table 2.** Fatigue failure scenarios [45].

| Scenario ID | Description | LOP [mm] |
|---|---|---|
| S1 | Full-length crack, partial penetration | 4 |
| S2 | Intermediate crack (width = 40 mm), partial penetration | 4 |
| S3 | Full-length crack, full penetration | 0.5 |
| S4 | Intermediate crack (width = 40 mm), full penetration | 0.5 |

The predicted fatigue life for all weld box setups and fatigue failure scenarios are given in Table 3.

**Table 3.** Estimated fatigue life (cycles) for each investigated design case according to [45].

| Fatigue Scenario | MTA | MTB | MTC | MTD | MTE | MTF |
|---|---|---|---|---|---|---|
| S1 | 102,841 | 287,933 | 1,103,500 | 67,768 | 33,366 | 96,467 |
| S2 | 589,198 | 1,538,700 | 5,486,300 | 458,650 | 182,450 | 517,390 |
| S3 | 311,108 | 925,034 | Infinite | 275,370 | 102,480 | 304,010 |
| S4 | 838,979 | 2,265,700 | Infinite | 664,850 | 255,420 | 731,070 |

### *7.2. Material Cost*

Material acquisition cost is calculated according to Equation (9) using material cost parameters in Table 4. Costs per kg material are here retrieved from steel price index figures [35] and other material data bases [36]. Production scrap rates are estimated from the ratio between cut-out size (including trimmings) and original feeding material size [47].

**Table 4.** Material cost data [35].

| Steel Type | Density [kg/m$^3$] | Cost [€/kg] | Scrap Rate [%] |
|---|---|---|---|
| Cold rolled, quenched and tempered, HSS plate | 7850 | 0.7 | 26 |
| Hot rolled HSS plate | 7850 | 0.65 | 6 |

Apart from used raw material, the cost of the weld filler material is also a factor. Filler material cost used is defined in Table 5.

**Table 5.** Weld filler material data.

| Filler Material | [€/kg] |
|---|---|
| ER 70S-6 | 5.3 |

### *7.3. Production Cost*

The production cost is a function of the manufacture of the plates and their assembly. The manufacture involves CNC-machining of HSS plate perimeters and cut-outs. The assembly involves mounting and weld tacking followed by several weld passes. It is assumed that the production is performed at an hourly labour cost of 4–5 € [48], and electricity fuselage annual cost of 3000 € for a 600 kW fuse [49]. To investigate the cost implication of introducing simple weld preparation and post-processing, manual cleaning is considered in both cases for the most involved production flow process. The process flow is specified in Figure 11. For more welding details, refer to [45,46,50].

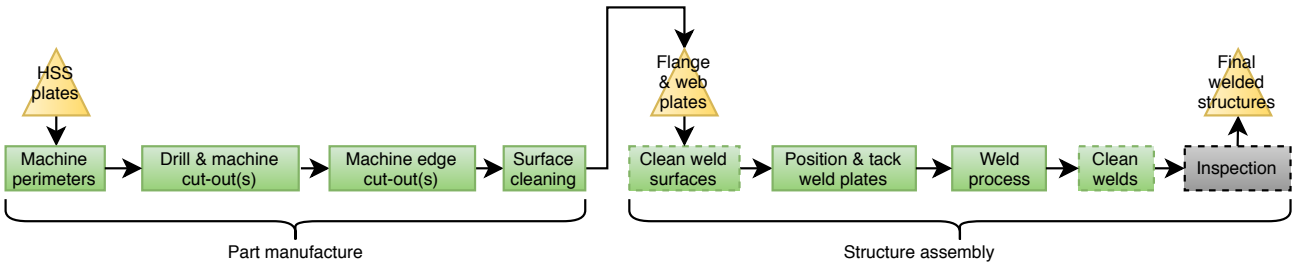


**Figure 11.** Welded box production flow. As the cost-impact of introducing weld preparation and weld post-processing is investigated, these processes are marked with a dashed line. Inspection cost is not the topic of this paper and is therefore excluded and marked in grey.

### *7.4. Use Phase Cost*

The use phase cost is a direct function of fatigue design together with application and governing duty cycle, or the proportion of time during which a piece of equipment is in active use. For a crane hoist, that means the proportion of time during which the hoist is lifting or lowering a load. Assuming a severe service [51], the crane hoist is estimated to operate in a harbour setting where it lifts containers weighing on average 25 tonnes. The crane hoist is estimated to lift 12 such containers per hour and is operated for 10 h a day, 250 days a year and has a technical lifetime of 20 years. The hoist crane is lifted using a 200 kW hoisting motor for all three cases. Continuous electricity cost is a function of the European weighted average electricity cost of 0.125 € per kwh [52] and required fuselage cost [23].

Apart from costs given by the explicit duty cycle, other use phase costs include inspections and maintenance. The American Occupational Safety and Health Administration [53] dictates that frequent and periodic inspections are to be carried out. Frequent, daily, inspections can be performed by the crane operator before use. In this paper, the costs of frequent inspections are implicitly recorded through assuming that visual inspections are

performed by the operator throughout the 10 h operating time. Periodic inspections are to be performed by experts, at a 1–12 month interval. In this paper periodic inspections by experts are considered to be performed annually. The annual inspection is expected to result in half a day shut-down and a cost resulting from the combination of downtime cost and expert inspection cost. The downtime cost corresponds to the explicit income loss of planned downtime. The income loss is considered to be the terminal handling charge (THC) loss, which range from 88–210 € for a 20 ft container [54]. In the performed PLCC, a THC-charge of 200 € as reported by Rotterdam, Netherlands [55] is used. The expert inspection cost fee is assumed equal to that of a flying dispatch cost [56], at an hourly rate of 85 € .

If fatigue failure or failure initiation is discovered during the technical lifetime of the crane hoist, repair and resulting downtime costs are also part of the life-cycle cost, see Figure 12. Similarly to that of annual inspection, it is assumed that a discovered failure requires half a day shut-down for repair work. Apart from the downtime and flying dispatch cost, the repair cost also includes the direct welding cost as calculated from the predictive technical cost model described in Section 5.2.2. The cumulative fatigue damage level, $C$, is evaluated over the estimated technical lifetime, and it is assumed that fatigue failure occurs if Miner's rule predicts a cumulative damage level of 70% according to

$$C = \frac{n_i S_i}{N_i S_i} > 0.7 \rightarrow fatigue\ failure \tag{11}$$

as a function of the comparative stress level, $S_i$, the current number of cycles, $n_i$ and the total number of cycles to failure, $N_i$, from Table 3. It is assumed that one fatigue cycle corresponds to the lifting of one container. The comparative stress level is given by geometry, gravity, flange plate mass, $m_i$, and representative flange plate area $A_i$, according to $\tan 45 g m_i / A_i$. If fatigue failure occurs, it is assumed that repair work resets the crane hoist to a fully operational, undamaged state ($n_i = 0$, $C = 0$).

### *7.5. End-of-Life Cost*

To allow for some alternative waste flows, a retrieval rate of 80% is accounted for at the final end-of-life stage. Production scrap is not credited to the full cycle, and is therefore simply treated as a cost. It is assumed that the steel of a retrieved component is valued at a UK market price of 0.26 € per kg [57].

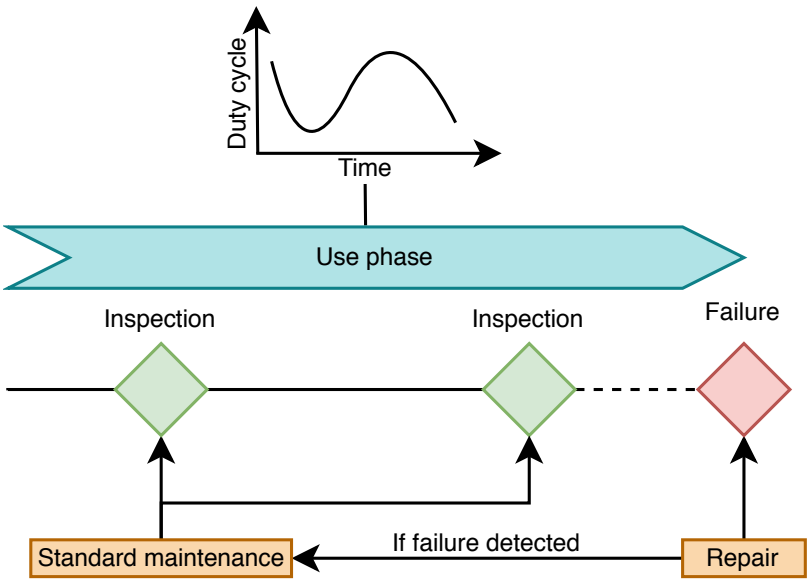


**Figure 12.** Important use phase costs include actual application use and resulting inspection, maintenance, repair and downtime.

## 8. Results

The results include sections on all investigated design cases. In addition, as the fatigue scenarios explored in the parametric PLCC concern the impact of weld penetration depth; a complementing pure production cost assessment is presented for three different penetration depths, $i$. These penetration depths are $i = 6, 8, 10$ mm, where 10 mm penetration depth corresponds to ideal full penetration. This assessment directly couples penetration depth to production cost and therefore shows how manufacturing efforts that ensure weld quality also drive production costs.

### *8.1. PLCC as a Function of Flange Plate Thickness, Web Plate Thickness and Hole Position*

The predicted life-cycle cost grow for each year, as presented in Figures 13–15 for each design case and fatigue scenario. The different design cases and fatigue scenarios show different step-wise incremental life-cycle cost increases over the years. These steps often correspond to repair and downtime costs as a result of fatigue damage, as shown by the R&I (research and inspection) label in the figures to the right in Figures 13–15. For the posed technical lifetime of 20 years, the initial production cost becomes negligible in all design cases. Different flange plate thicknesses (MTA-MTC) and shifted hole position (MTE-MTF) have the highest impact on the overall lifecycle cost, see Figures 13 and 15, respectively. A lowered web thickness (MTD), is shown in Figure 14, to have little effect on the overall lifecycle cost for all fatigue scenarios.

The flange plate thickness is in Figure 13 shown to have a high impact on the lifecycle cost, and most dominantly so in the most severe fatigue scenario, S1. At full technical life, increasing the flange thickness 10 mm (MTB) reduces the overall lifecycle cost by 40%, while increasing the flange thickness 30 mm (MTC) reduces the lifecycle cost by 60%. In the same fatigue scenario, it can be noted that repairs for the cases with increased flange thicknesses, MTB and MTC, are needed each third and ninth year, respectively. The baseline on the other hand, needs continuous annual repairs throughout its lifetime for the same fatigue scenario. For the other three fatigue scenarios, S2–S4, increased flange plate thicknesses also result in reduced lifecycle costs and less frequent repairs.

Thinner web plates are shown to have low impact on the life-cycle cost of the full box, see Figure 14. For the fatigue scenarios S1 and S3, we find that all considered cases need annual repairs thus making the design cases equal in terms of life-cycle cost. A small impact can be noticed in the less severe fatigue scenarios, S2 and S4, where the life-cycle cost at full technical life is a few percentage higher for the case with thinner webs. In each fatigue scenario, the thinner webs case, MTD, need to be repaired with one respectively two years shorter intervals compared to the baseline box.

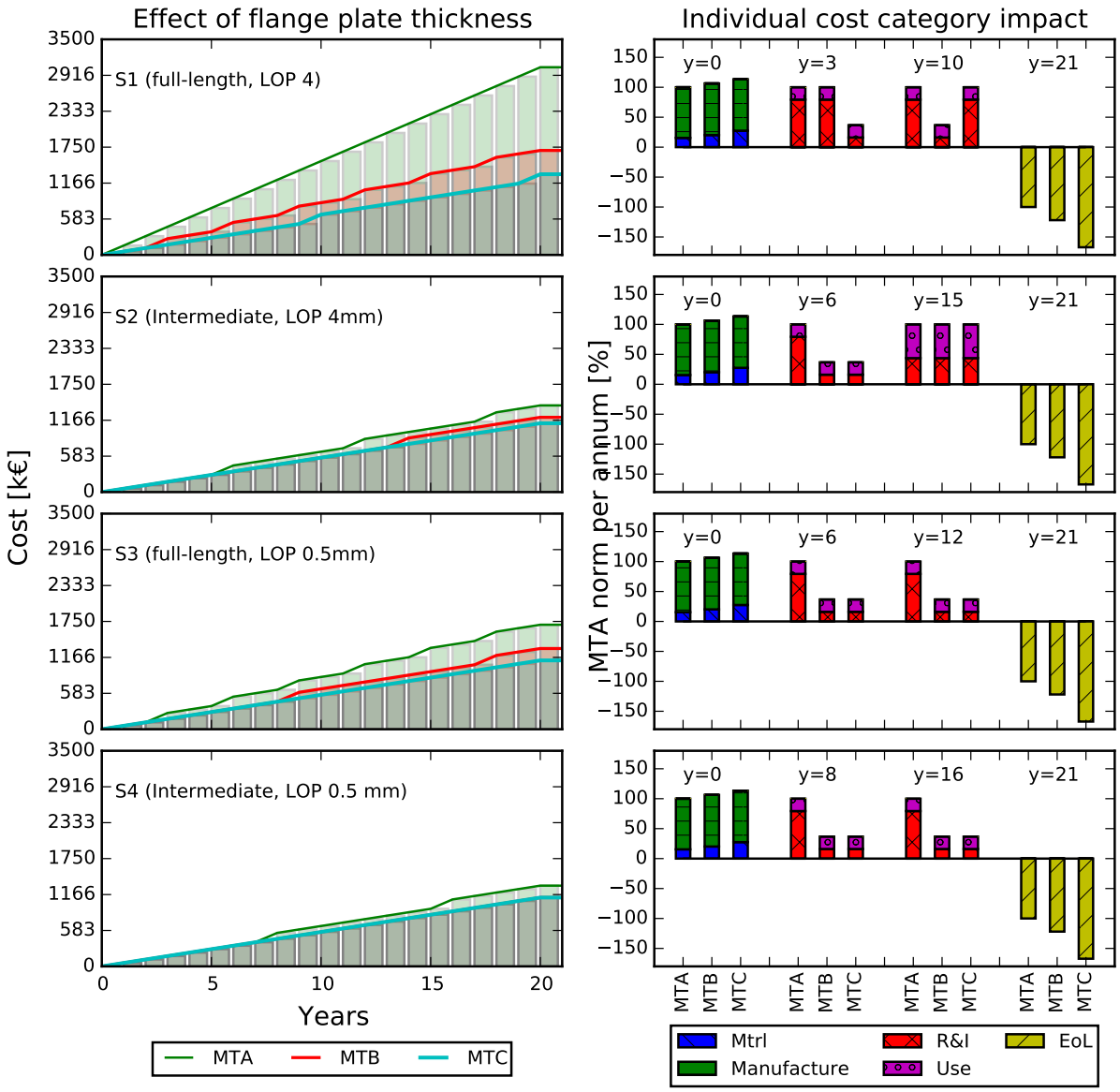


**Figure 13.** Annual accumulated lifecycle cost for each fatigue scenario and design cases MTA-MTC, in which flange thickness is varied according to $t_f = 30, 40, 60$ mm, respectively. (**left**) accumulated costs per year. (**right**) the divisions between cost contributions for specified year, normalized with respect to the baseline case (MTA).

The position of the hole on the flange plates is shown in Figure 15 to have high impact on the fatigue scenarios S2–S4. For the most severe fatigue scenario, S1, we find that all considered cases need annual repairs. The highest impact of eccentricity is shown in fatigue scenario S3, where the life-cycle cost becomes close to 70% higher as opposed to the baseline box. In all fatigue scenarios it is shown that increasing the flange thickness by 10 mm, case MTF, compensates for the hole eccentricity. Thus, in all fatigue scenarios case MTF returns a similar life-cycle cost as that of the baseline box.

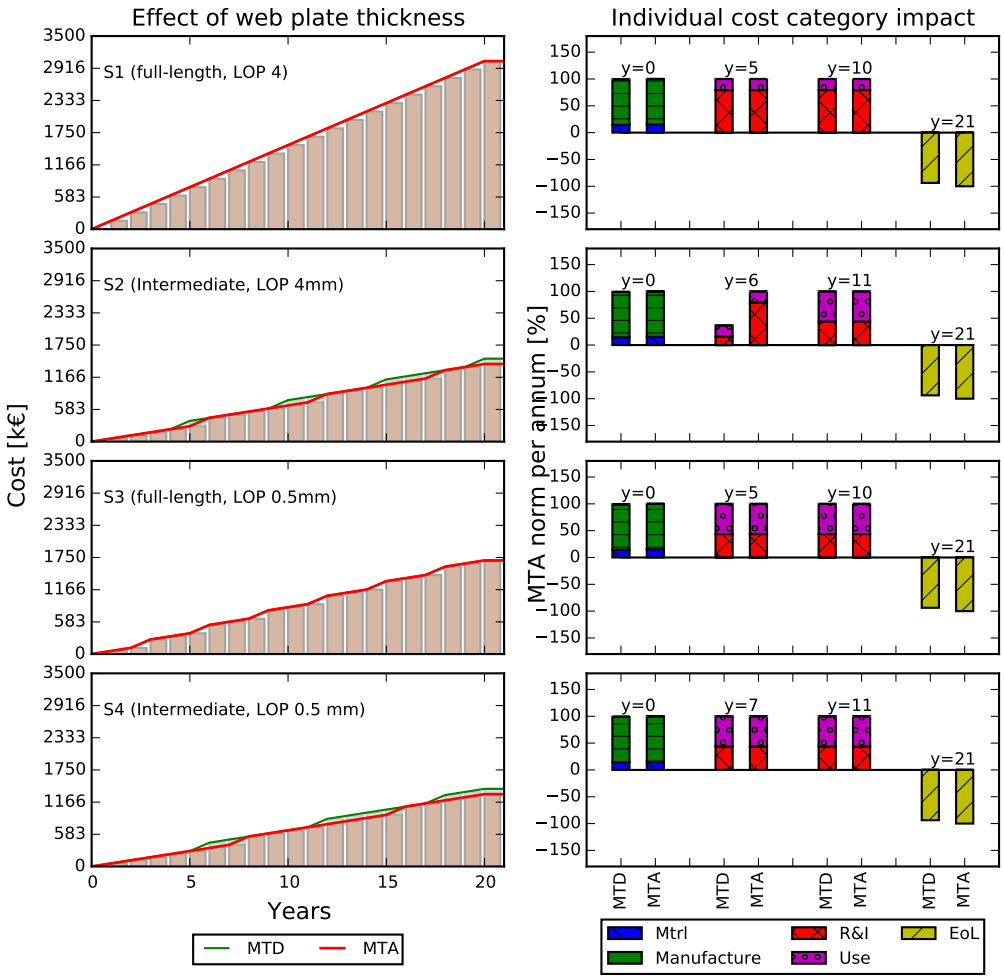


**Figure 14.** Annual accumulated life-cycle cost for each fatigue scenario and design cases MTA and MTD, in which the web plate thickness is varied according to $t_w = 8, 10$ mm, respectively. (**left**) accumulated costs per year. (**right**) the divisions between cost contributions for specified year, normalized with respect to the baseline case (MTA).

## Production Cost

The production cost of the welded box as a function of annual manufacturing volume for each flange plate thickness case is given in Figure 16. The production cost reduces with increasing annual manufacturing volume. This is a result of how the cost for lower annual manufacturing volume is dominated by manufacturing and indirect costs such as investments, see Figure 17. For larger annual manufacturing volumes, the production cost stabilize at a lowest cost per part, which corresponds to a stable division between cost categories, governed by direct costs such as material and operator costs. When the lowest stable cost has been reached, a flange plate thickness increase of 10 mm increases the production cost with 24% while a flange plate thickness increase of 20 mm increases the production cost with 43%.

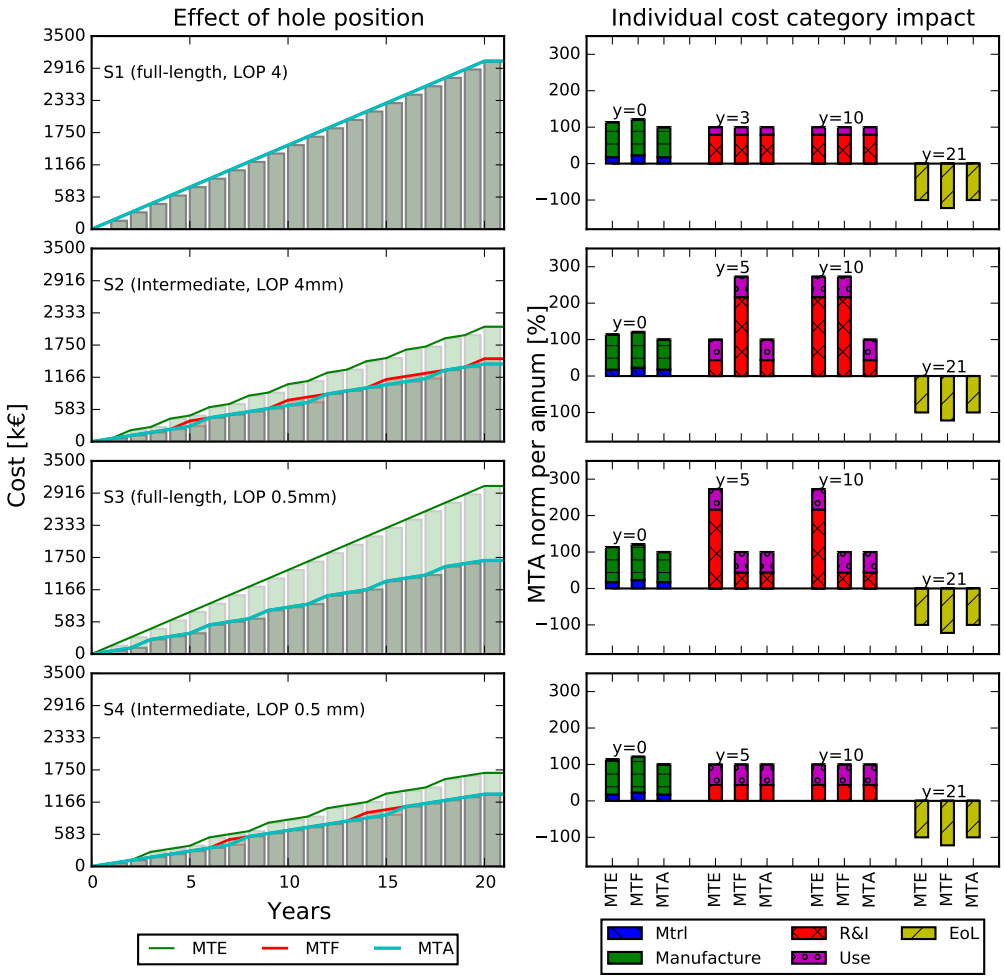


**Figure 15.** Annual accumulated life-cycle cost for each fatigue scenario and design cases MTE, MTF and MTA, where each represents a different hole position (eccentric vs. centric). (**left**) accumulated cost for per year. (**right**) the divisions between cost contributions for specified year, normalized with respect to the baseline case (MTA).

How the cost shifts importance between indirect costs (investments and facility costs) to direct costs (operator, material and direct electricity costs) is similarly shown for the process of assembly, i.e., welding, of the box structure, shown in Figure 18.

### *8.2. The Impact of Penetration Depth on Production Cost*

The production costs as a function of annual manufacturing volume of the welded box structure for different penetration depths are given in Figure 19. It is clear that only accounting for different penetration depths, or in fact different bead mass, has little impact on the overall production cost. However, to ensure full penetration depth, the welding process need to be more involved. If considering increased effort through applying pre- and post-weld cleaning and assuming previous hourly labour rates, the cost increases between 16–30% depending on the rate of cleaning, see Figure 19.

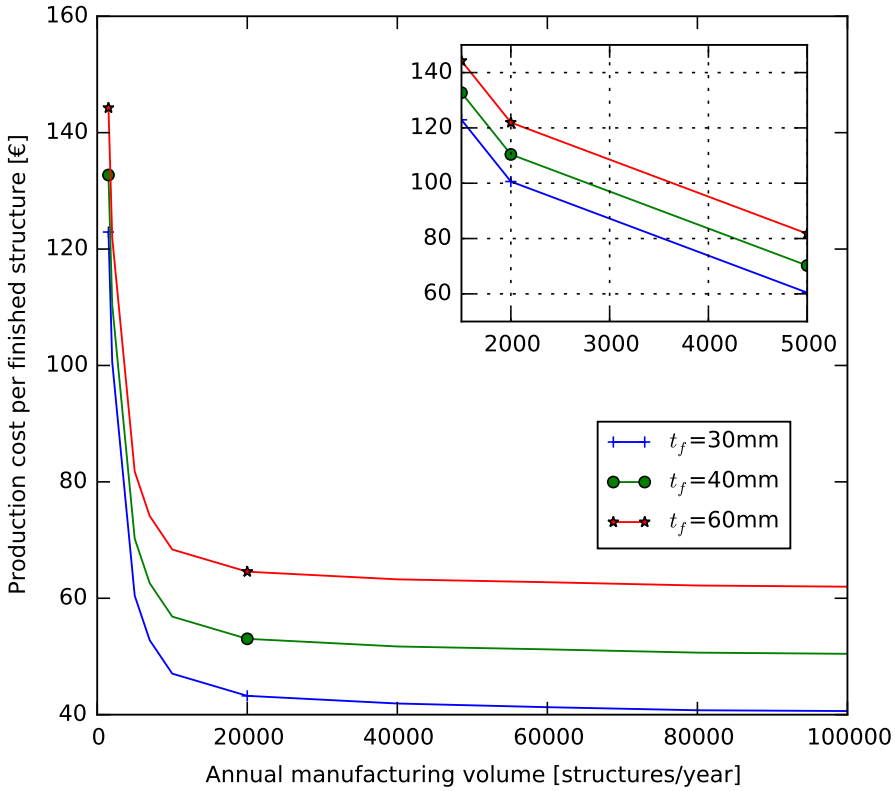


**Figure 16.** Production cost as a function of annual manufacturing volume for cases $t_f = 30, 40, 60$ mm.

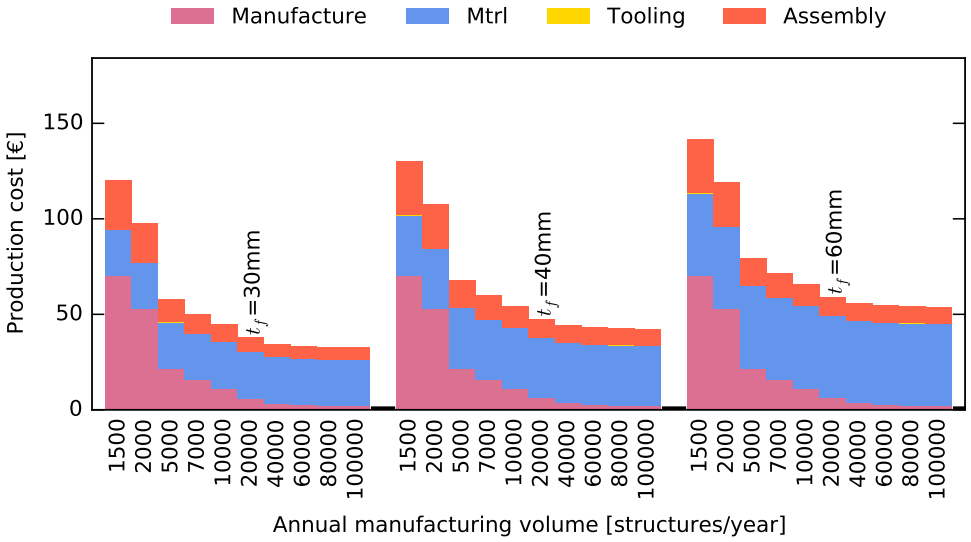


**Figure 17.** Cost division between manufacture, material and assembly (i.e., welding) costs for different annual manufacturing volumes for the case of $t_f = 30, 40, 60$ mm.

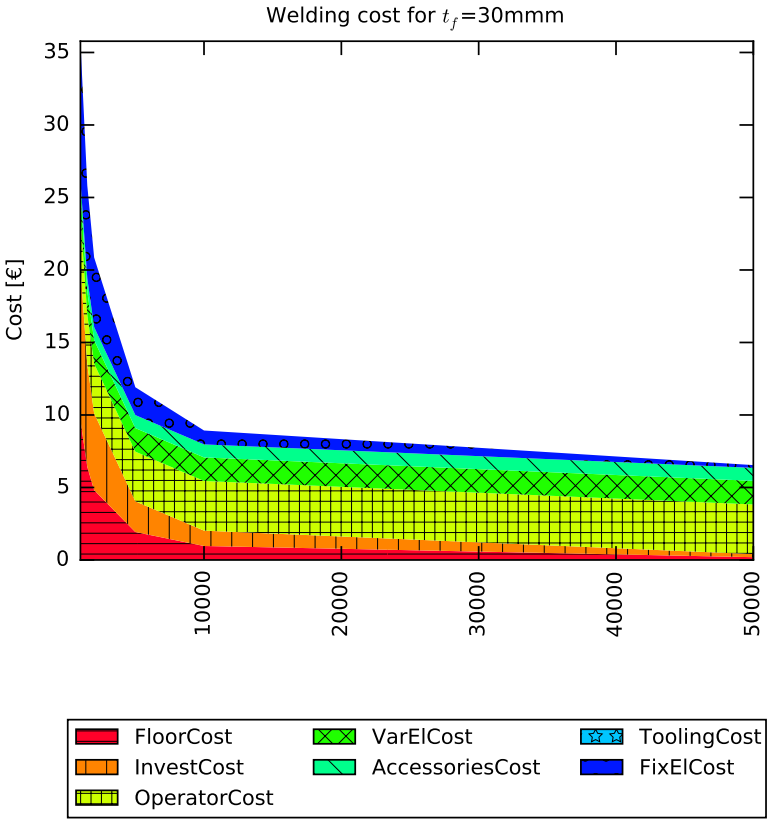


**Figure 18.** Cost division between cost categories for the welded box assembly, i.e., welding, for the case of $t_f = 30$ mm.

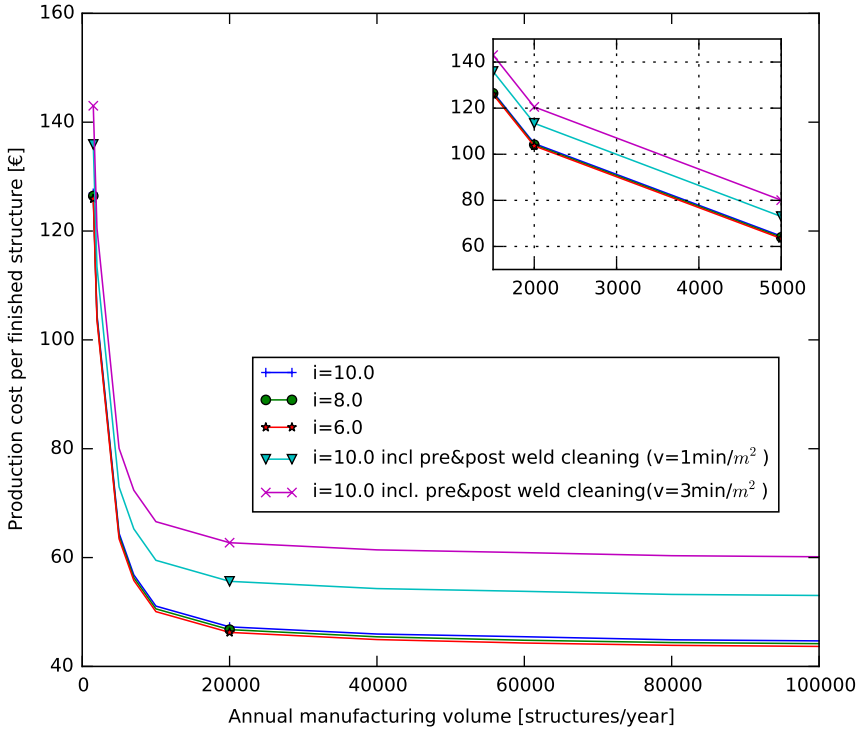


**Figure 19.** Production cost as a function of annual manufacturing volume for different penetration depths together with pre- and post-weld cleaning $i = 6, 8, 10$ mm.

## 9. Discussion

The presented PLCC scheme and case study have shown the importance of proper design and fatigue assessment in an early conceptual design stage in order to ascertain an optimized design and control life-cycle costs. Furthermore, the fact that maintenance and repair costs in the most severe fatigue scenarios tend to drive the life-cycle costs highlights the importance to properly control and inspect manufacturing variations present in welding.

The life-cycle assessment has demonstrated that the most important life-phase is the operational use and that the costs to minimize are operation, maintenance and repair. Ultimately, the size of the use phase costs in comparison to the production costs means most fatigue-enhancing efforts, such as increasing the thickness of the load-carrying member ($t_f$), change of steel steel grade used or introducing improved weld classes, are justified even when resulting in significantly increased production costs. When increasing the flange thickness for example, a 20 mm flange plate thickness increase comes at a cost of 43% production cost increase (or about 18 €), which results in a 60% overall life-cycle cost reduction (or about 1.75 M€). Efforts addressed at managing manufacturing variations, such as flange hole position eccentricity, can similarly also have beneficial impact on the overall lifecycle cost of a design. For example, the impact of the flange hole position eccentricity is in design case MTF shown to be fully compensated by a flange plate thickness increase of 10 mm.

However, it is important to express that minimized production costs are needed to ensure a competitive supply chain and final component. This means all design improvements that maximise the structure fatigue life of a welded structure need to be evaluated for their efficiency before implemented. For example, although ensuring consistent penetration depth is key to improved fatigue behaviour, different strategies to achieve this are more or less costly. For example, the simple introduction of pre- and post-cleaning has been shown to have a large impact on the final, stabilized, production cost, resulting in production cost increases of 16-30% for large annual manufacturing volumes. Thus, to avoid implementing a fatigue improvement strategy that is less cost-efficient than another, predictive technical cost modelling and cost assessment becomes valuable tools.

The welding extension added to the used predictive technical cost model has been verified to that of actual weld specification documents, and the predicted weld time has been shown to comply well with that of recorded figures. This means the estimated production costs are accurately sized. However, it is important to note that the final production costs are a function of defined process scheme and indeed, country of manufacture. Particularly operator and electricity costs vary greatly between nations.

Finally it is important to emphasize that the incorporation of life-cycle costing in an early design stage is not only beneficial from a design perspective, but will also be a key driving factor towards enabling future circular economy, and indeed a fully sustainable production system.

*View of Variation*

The variation in production can be viewed differently depending on the different stages of the product development stage and role dependent; different roles within the organization needs different information, hence context dependent. In the manufacturing flow, the variation could occur between factories, technology suppliers, batches and within one part. Variation could also be observed within one single weld; along the weld, within the cross section and weld toe geometry. Hence, variation will occur in all product development phases which will have a significant impact on the product quality. Therefore, it is important to identify the sources of variations in the different product development phases in order to minimize their cause. Figure 20 illustrates examples of different sources of variation that could occur in the welding production.

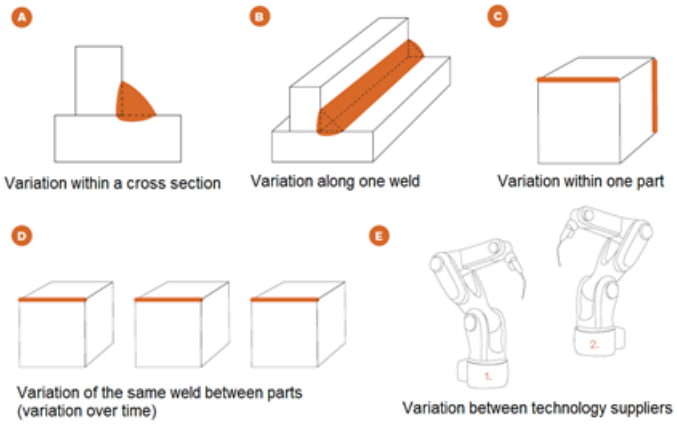


**Figure 20.** Different sources of variation (**A**–**E**).

## 10. Conclusions

Presented PLCC method and case study have shown the importance of designing a welded structure with respect to structural demands and variation in manufacture and corresponding predicted life-cycle cost. In addition, used predictive technical cost model has been demonstrated valuable for investigating the cost-efficiency of fatigue-enhancing strategies of the same welded structure. Some important conclusions are:

- Welding and production costs are negligible in relation to re-occurring repair costs for all considered design cases and fatigue scenarios.
- Repair and maintenance costs outweighs that of operational costs for the more severe fatigue scenarios considered.
- Increased flange plate thicknesses is the most effective means to reduce overall life-cycle costs, as it can increase the intervals between repairs significantly. Ultimately, increased flange plate thicknesses can result in lifecycle cost reductions of up to 60% (or about 1.75 M€) and fully compensate for hole position variations considered.

**Author Contributions:** Conceptualization, M.K.H. and M.K.; methodology, M.K.H.; software, M.K.H.; validation, M.K.H., M.K. and Z.B.; formal analysis, M.K.H.; investigation, M.K.H.; resources, M.K.H.; data curation, M.K.H.; writing—original draft preparation, M.K.H. and Z.B.; writing—review and editing, Z.B., M.K. and M.Å.; visualization, M.K.H. and M.K.; supervision, M.Å. and Z.B.; project administration, M.K.H and Z.B; funding acquisition, M.K.H, Z.B. and M.K. All authors have read and agreed to the published version of the manuscript.

**Funding:** This work was supported by the Centre for ECO2 Vehicle Design, funded by the Swedish Innovation Agency Vinnova (Grant Number 2016-05195) and the project VariLight, funded by the Swedish Innovation Agency Vinnova through Grant Number 2016-03363.

**Institutional Review Board Statement:** Not applicable.

**Informed Consent Statement:** Not applicable.

**Data Availability Statement:** The data presented in this study are available within the article itself, drawing on provided reference list.

**Conflicts of Interest:** The authors declare no conflict of interest.

## References

1. Öberg, A.E.; Åstrand, E. Improved productivity by reduced variation in gas metal arc welding (GMAW). *Int. J. Adv. Manuf. Technol.* **2017**, *92*, 1027–1038. [CrossRef]
2. Hobbacher, A. *Recommendations for Fatigue Design of Welded Joints and Components*, 2nd ed.; IIW Collection; Springer: Berlin/Heidelberg, Germany, 2016. [CrossRef]
3. Radaj, C.D.; Fricke, W. *Fatigue Assessment of Welded Joints by Local Approaches*, 2nd ed.; Woodhead Publishing Limited: Sawston, UK, 2006.
4. Fricke, W. IIW guideline for the assessment of weld root fatigue. *Weld. World* **2020**, *57*, 753–791. [CrossRef]

5. Frank, K.H.; Fisher, J.W. Fatigue strength of fillet welded cruciform joints. *J. Struct. Div.* **1979**, *105*, 1727–1740. [CrossRef]
6. Guha, B. A new fracture mechanics method to predict the fatigue life of welded cruciform joints. *Eng. Fract. Mech.* **1995**, *52*, 215–229. [CrossRef]
7. Marquis, G.B. ; Barsoum, Z. *IIW Recommendations for the HFMI Treatment For Improving the Fatigue Strength of Welded Joints*; Springer: Singapore, 2016; ISBN 978-981-10-2503-7.
8. Aldén, R.; Barsoum, Z.; Vouristo; T.; Al-Emrani, M. Robustness and effect of weld quality on the fatigue life improvement of welded joints using HFMI techniques. *Weld World* **2020**, *64*, 1947–1956. [CrossRef]
9. Yekta, R.T; Ghahremani,K.; Walbridge, S. Effect of quality control parameter variations on the fatigue performance of ultrasonic impact treated welds. *Int. J. Fatigue* **2013**, *55*, 245-256. [CrossRef]
10. Silva,F.J.G.; Pinho, A.P; Pereira, A.B.; Paiva, O.C. Evaluation of Welded Joints in P91 Steel under Different Heat-Treatment Conditions. *Metals* **2020**, *10*, 99. [CrossRef]
11. Sousa, V.F.C.; Silva,F.J.G.; Pinho, A.P.; Pereira, A.B.; Paiva, O.C. Enhancing Heat Treatment Conditions of Joints in Grade P91 Steel: Looking for More Sustainable Solutions. *Metals* **2021**, *11*, 495. [CrossRef]
12. Hagnell, M.K.; Åkermo, M. Cost efficiency, integration and assembly of a generic composite aeronautical wing box. *Compos. Struct.* **2016**, *152*, 1014–1023. [CrossRef]
13. Rybicka, J.; Purse, T.; Parlour, B. A Generic Cost Estimating Approach for a Composite Manufacturing Process Assessment. *Adv. Manuf. Technol. XXXIV* **2021**. [CrossRef]
14. Tierney, C.; Higgins, C.; Quinn, D.; Backer, J.D.; Allen, C.; Örtnäs, A.; Persson, J.; McClelland, J.; Higgins, P.; Murphy, A. A scalable cost modelling architecture for evaluating the production cost-effectiveness of novel joining techniques for aircraft structures. *Procedia Manuf.* **2021**, *54*, 7–12. [CrossRef]
15. Bouchouireb, H.; O'Reilly, C.J.; Göransson, P.; Schöggl, J.P.; Baumgartner, R.J.; Potting, J. Towards Holistic Energy-Efficient Vehicle Product System Design: The Case for a Penalized Continuous End-of-Life Model in the Life Cycle Energy Optimisation Methodology. *Proc. Des. Soc. Int. Conf. Eng. Des.* **2019**, *1*, 2901–2910. [CrossRef]
16. Poulikidou, S.; Schneider, C.; Björklund, A.; Kazemahvazi, S.; Wennhage, P.; Zenkert, D. A material selection approach to evaluate material substitution for minimizing the life cycle environmental impact of vehicles. *Mater. Des.* **2015**, *83*, 704–712. [CrossRef]
17. Penadés-Plà, V.; García-Segura, T.; Martí, J.V.; Yepes, V. An Optimization-LCA of a Prestressed Concrete Precast Bridge. *Sustainability* **2018**, *10*, 685. [CrossRef]
18. Lee, K.M.; Cho, H.N.; Choi, Y.M. Life-cycle cost-effective optimum design of steel bridges. *J. Constr. Steel Res.* **2004**, *60*, 1585–1613. [CrossRef]
19. Zou, G.; Banisoleiman, K.; González, A. Probabilistic maintenance optimization for fatigue-critical components with constraint in repair access and logistics. In Proceedings of the 14th International Conference on Probabilistic Safety Assessment and Management (PSAM 14), Los Angeles, CA, USA, 16–21 September 2018.
20. Kim, S.; Frangopol, D.M.; Soliman, M. Generalized Probabilistic Framework for Optimum Inspection and Maintenance Planning. *J. Struct. Eng.* **2013**, *139*, 435–447. [CrossRef]
21. Kim, S.; Ge, B.; Frangopol, D.M. Effective optimum maintenance planning with updating based on inspection information for fatigue-sensitive structures. *Probabilistic Eng. Mech.* **2019**, *58*, 103003. [CrossRef]
22. Turan, O.; Ölçer, A.İ.; Lazakis, I.; Rigo, P.; Caprace, J.D. Maintenance/repair and production-oriented life cycle cost/earning model for ship structural optimisation during conceptual design stage. *Ships Offshore Struct.* **2009**, *4*, 107–125. [CrossRef]
23. Hagnell, M.K.; Åkermo, M. A composite cost model for the aeronautical industry: Methodology and case study. *Compos. Part B Eng.* **2015**, *79*, 254–261. [CrossRef]
24. Öberg, A.E. VariLight Reduced VARIation in the manufacturing processes enabling LIGHTweight welded structures, public report. *Fordonsstrategisk Forsk. Och Innov.* **2019**.
25. Broadbent, C. Steel's recyclability: demonstrating the benefits of recycling steel to achieve a circular economy. *Int. J. Life Cycle Assess* **2016**, *21*, 1658–1665. [CrossRef]
26. Worrel, E.; Reuter, M.A. (Eds.) *Handbook of Recycling*; Elsevier: Amsterdam, The Netherlands, 2014.
27. Harvey, L.D.D. Iron and steel recycling: Review, conceptual model, irreducible mining requirements, and energy implications. *Renew. Sustain. Energy Rev.* **2021**, *138*, 110553. [CrossRef]
28. Hagnell, M.K. Technical Cost Modelling and Efficient Design of Lightweight Composites in Structural Applications. Ph.D. Thesis, KTH Royal Institute of Technology, Stockholm, Sweden, 2019.
29. Foundation, P.S. Python Language Reference, Version 2.7. Available online: http://www.python.org (accessed on 31 March 2021).
30. Coromant, S. Milling Formulas and Definitions. Available online: https://www.sandvik.coromant.com/en-gb/knowledge/machining-formulas-definitions/pages/milling.aspx (accessed on 31 March 2021).
31. SSAB. Machining Recommendations for Strenx®. Available online: https://www.ssab.com/support/processing#downloads (accessed on 24 September 2021).
32. Weman, K. *Welding Processes Handbook*, 2nd ed.; Woodhead Publishing: Sawston, UK, 2012.
33. Jarmai, K.; Farkas, J. Cost calculation and optimisation of welded steel structures. *J. Constr. Steel Res.* **1999**, *50*, 115–135. [CrossRef]
34. Zhu, J.; Khurshid, M.; Barsoum, Z. Accuracy of computational welding mechanics methods for estimation of angular distortion and residual stresses. *Weld. World* **2019**, *63*, 1391–1405. [CrossRef]

35. MEPS International Ltd. World Steel Prices. Available online: https://worldsteelprices.com/; https://www.meps.co.uk/gb/en/products/europe-steel-prices (accessed on 31 March 2021).
36. London Metal Exchange (LME). Metal Prices. Available online: https://www.lme.com/ (accessed on 31 March 2021).
37. Maes, J. Make It from Metal. Available online: https://makeitfrommetal.com/how-much-does-a-cnc-machine-cost/ (accessed on 31 March 2021).
38. EWM AG. Welding Machines. Available online: https://www.ewm-sales.com/ (accessed on 31 March 2021).
39. The Indiana Oxygen Company. Welding Supplies from Ioc. Available online: https://www.weldingsuppliesfromioc.com/ (accessed on 31 March 2021).
40. BS7608. *Guide to Fatigue Design and Assessment of Steel Products, 2014–2015*, 2nd ed.; BSI Standards: London, UK, 2015.
41. EN1993-1-9. *Eurocode 3: Design of STEEL structures—Part 1–9: Fatigue, 2003*; BSI Standards: London, UK, 2003.
42. EN13001. *Cranes—General design—Part 1: General Principles and Requirements, 2015*; BSI Standards: London, UK, 2015.
43. Pettersson, G.; Barsoum, Z. Finite element analysis and fatigue design of a welded construction machinery component using different approaches. *Eng. Fail. Anal.* **2012**, *26*, 274–284. [CrossRef]
44. Hultgren, G.; Khurshid, M.; Haglund, P.; Barsoum, Z. Mapping of scatter in fatigue life assessment of welded structures—A round robin study. *Weld. World* **2021**, *65*, 1841–1855. [CrossRef]
45. Delkhosh, E.; Khurshid, M.; Barsoum, I.; Barsoum, Z. Fracture mechanics and fatigue life assessment of box-shaped welded structures: FEM analysis and parametric design. *Weld. World* **2020**, *64*, 1535–1551. [CrossRef]
46. Zhu, J.; Khurshid, M.; Barsoum, Z. Assessment of computational weld mechanics concepts for estimation of residual stresses in welded box structures. *Procedia Struct. Integr.* **2019**, *17*, 704–711. [CrossRef]
47. Kaltenbach. The Scrap Calculation in a CNC Plate Processing Line. Available online: https://www.kaltenbach.com/en/media/talking-steel/the-scrap-calculation-in-a-cnc-plate-processing-line/ (accessed on 31 March 2021).
48. Eurostat. Hourly Labour Costs. Available online: https://ec.europa.eu/eurostat/statistics-explained/index.php?title=Hourly_labour_costs (accessed on 20 September 2021).
49. The World Bank. Available online: https://www.worldbank.org/ (accessed on 31 March 2021).
50. Haglund, M.K.P.; Barsoum, Z. Mapping of scatter in fatigue life assessment of welded structures—A Round Robin Study. In Proceedings of the IIW Annual Assembly and International Conference, Bratislava, Slovakia, 7–12 July 2019.
51. Acculift. Demystifying The Duty Cycle of a Hoist. Available online: https://acculift.com/demystifying-the-duty-cycle-of-a-hoist/ (accessed on 20 September 2021).
52. Eurostat. Electricity Price Statistics. Available online: https://ec.europa.eu/eurostat/statistics-explained/index.php?title=Electricity_price_statistics (accessed on 20 September 2021).
53. Occupational Safety and Health Administration (OSHA). 1910.179—Overhead and Gantry Cranes. Available online: https://www.osha.gov/laws-regs/regulations/standardnumber/1910/1910.179 (accessed on 31 March 2021).
54. European Commission Competition. Terminal Handling Charges during and after the Liner Conference Era. Available online: https://ec.europa.eu/competition/sectors/transport/reports/terminal_handling_charges.pdf (accessed on 31 March 2021).
55. Container News. ZIM Updates THC/THD Rates. Available online: https://container-news.com/zim-updates-thc-thd-rates/ (accessed on 31 March 2021).
56. Mazzella Companies. Lifting & Rigging Learning Center. Available online: https://www.mazzellacompanies.com/Resources/Blog/how-much-does-an-overhead-crane-inspection-cost (accessed on 20 September 2021).
57. Free Encyclopedia for UK Steel Construction Information. Recycling and Reuse. Available online: https://www.steelconstruction.info/Recycling_and_reuse (accessed on 3 March 2021).